Received: 5 April 2019 | Revised: 17 June 2019 | Accepted: 13 July 2019

DOI: 10.1002/we.2401

RESEARCH ARTICLE

WILEY

A study of modal damping for offshore wind turbines considering soil properties and foundation types

Takeshi Ishihara | Lilin Wang

Department of Civil Engineering, School of Engineering, The University of Tokyo, Tokyo, Japan

Correspondence
Lilin Wang, Department of Civil Engineering, School of Engineering, The University of Tokyo, 7-3-1, Hongo, Bunkyo-ku, Tokyo, Japan.
Email: lilin.wang@bridge.t.u-tokyo.ac.jp

Abstract

The modal damping ratio for each mode is crucial to characterize the dynamic behavior of offshore wind turbines and widely used by simulation software in wind turbine engineering, such as Bladed and FAST. In this study, modal damping ratios of offshore wind turbines are systematically studied for different soil properties and foundation types. Firstly, the modal damping ratios and modal frequencies for the first and second modes of a gravity foundation–supported offshore wind turbine are studied. An offshore wind turbine supported by a monopile foundation is then investigated to clarify the characteristics of modal damping ratios and modal frequencies for the monopile foundation. The soil parameters are identified by means of genetic algorithm (GA). Predicted modal damping ratios and modal frequencies as well as modal shapes show good agreement with the field measurements for both foundations. Finally, a sensitivity analysis study is carried out to investigate the effects of soil properties and foundation types on modal damping ratios. For the gravity foundation–supported offshore wind turbine, soil properties affect the modal damping ratio of the second mode largely, but affect that of the first mode little, while for the monopile-supported offshore wind turbine, soil properties affect the modal damping ratios of the first and second modes significantly. Predicted natural periods and modal damping ratios of the first mode for both foundations by a pair of simple models agree well with those by numerical models.

KEYWORDS

GA based identification, gravity foundation, modal damping, monopile foundation, Offshore wind turbine, soil properties

1 | INTRODUCTION

The modal damping ratio is the ratio of actual damping to critical damping, which is crucial to characterize the dynamic behavior of offshore wind turbines and is widely used by simulation software in wind turbine engineering, such as Bladed[1] and FAST.[2] The modal damping ratios of wind turbines are usually determined according to the recommendations in the design guidelines. However, as mentioned in Oh and Ishihara,[3] the recommended values of the structural damping ratios vary largely among different design codes, such as ASCE and AWEA,[4] JSCE guidelines for design of wind turbine support structures and foundations,[5] IEC61400-1,[6] and German guideline for wind turbines.[7] They explained that this variation depends on wind turbine sizes and proposed an empirical formula of the structural damping ratios of the first mode for wind turbines with steel towers, based on a 65-kW wind turbine,[8] a 400-kW wind turbine,[9] and a 2.4-MW wind turbine.[3] One problem is how to evaluate the modal damping ratio of the first mode

The peer review history for this article is available at https://publons.com/publon/10.1002/we.2401

because the soil property such as S-wave velocity and Poisson ratio may affect that. Another problem is the lack of experimental data for the modal damping ratios of the second mode of wind turbines, since the frequency of the second mode is usually in the range where it is difficult to excite by human excitations or emergency stops.

Recently, modal damping ratios of offshore wind turbines have been studied by means of field measurements. Oh and Ishihara[3] performed a series of excitation tests on a 2.4-MW offshore wind turbine supported by a gravity foundation using an active mass damper, which measured modal frequencies, modal damping ratios, and modal shapes of both first and second modes. The results of excitation tests show that the modal damping ratio of the first mode is 0.2%, while that of the second mode is 2.4%. They explained that the modal damping ratio of the first mode is nearly equal to structural damping ratio of the first mode, assuming the contribution from the soil under the gravity foundation to the modal damping ratio of the first mode is negligible because the soil underneath the foundation is stiff rock, but they did not explain why the modal damping ratio of the second mode increases. They also predicted the modal shapes of the first and second modes by a fixed-foundation model (FF model) and compared with those measured by five accelerometers. The predicted modal shape presented favorable agreement with the measurement for the first mode, but illustrated difference near the foundation for the second mode.

For piled offshore support structures, GL[10] summarized the studies by Cook and Vandiver[11] and Tarp-Johansen et al[12] and recommended that the overall damping was in the range of 0.8% to 1.2%, which was defined as the summation of material damping of steel and soil damping due to inner soil friction. Recently, the signals during emergency shutdown of offshore wind turbines supported by monopile foundations were analyzed to estimate the modal damping of the first mode after subtracting aerodynamic and hydrodynamic damping. The modal damping ratio of the first mode was found in the range of 0.85% to 1.19%, which includes the contribution from structural damping and soil damping and is within the same range as shown in GL.[10] The contribution of soil damping is back-calculated after assuming structural damping ratio. Damgaard et al[13] mentioned that the structural damping ratio was 0.19% and the soil damping was 1% for the first mode, while Shirzadeh et al [14] assumed that the structural damping ratio was 0.6% and the soil damping was 0.25% for the first mode. Obviously, the structural damping ratio of the first mode in Damgaard et al[13] is close to that measured by Oh and Ishihara (2018)[3] for a gravity foundation, but that in Shirzadeh et al[14] is not. This indicates that the structural damping ratio of the first mode for the steel tower is independent on the type of foundation and has a value as shown by Oh and Ishihara.[3]

In this study, modal damping ratios of offshore wind turbines are systematically studied for different soil properties and foundation types. Numerical models for the gravity and monopile foundations, eigenvalue analysis, free decay analysis, and GA-based identification are described in Section 2. The modal damping ratios of the first and second modes as well as modal frequencies and modal shapes for a 2.4-MW offshore wind turbine supported by the gravity foundation and a 3-MW offshore wind turbine supported by the monopile foundation are then investigated and compared with those obtained from the field measurements in Section 3. Finally, a sensitivity analysis study is carried out to investigate the effects of soil properties and foundation types on modal damping ratios for the first and second modes and a pair of simple models to predict the natural periods and modal damping ratios of the first mode for offshore wind turbines are evaluated in Section 4. Conclusions are given in Section 5.

2 | NUMERICAL MODEL

Numerical models for the gravity and monopile foundations are given in Sections 2.1 and 2.2, eigenvalue analysis and free decay analysis are described in Sections 2.3 and 2.4, and GA-based identification is defined in Section 2.5.

2.1 | SR model for gravity foundation

The gravity foundation–supported wind turbine is modelled by sway-rocking model (SR model) as shown in Figure 1. In SR model, the rotor-nacelle assembly is modelled with a lumped mass and connetted to the tower top by using a rigid beam. The tower and the substructure are modelled with the lumped masses and the Euler-Bernoulli beam elements. The number of tower beam elements is 24, which follows the suggestion of JSCE.[5] All lumped masses and beam stiffnesses are determined according to the real wind turbine. The structural damping ratio of the first mode is determined according to the empirical formula proposed by Oh and Ishihara (2018).[3] The structural damping ratio of the second mode uses the same value as that of the first mode as recommended by JSCE.[5] The gravity foundation is modelled by a lumped mass at the ground level and connected to the substructure base by using a rigid beam, and the soil-structure interaction is modelled by a pair of springs and dashpots in the sway and rocking directions at the ground level. This study focuses on the modal damping ratios for the dynamic analysis under wind and wave conditions. The modal damping ratios of the first and second modes are investigated by using linear soil springs and dashpots for each case. The structural damping ratios for higher modes can be calculated using Rayleigh damping model. The same idea is used for the monopile foundation as shown in Section 2.2.

The spring stiffness values and dashpot damping values for the sway motion (K_S, C_S) and for the rocking motion (K_R, C_R) are calculated by the nondimensional dynamic impedance $K_{j0}(\omega)$ as

$$K_{j0}(\omega) = K_{j0}^{\text{real}} + \ iK_{j0}^{\text{imag}}, \tag{1}$$

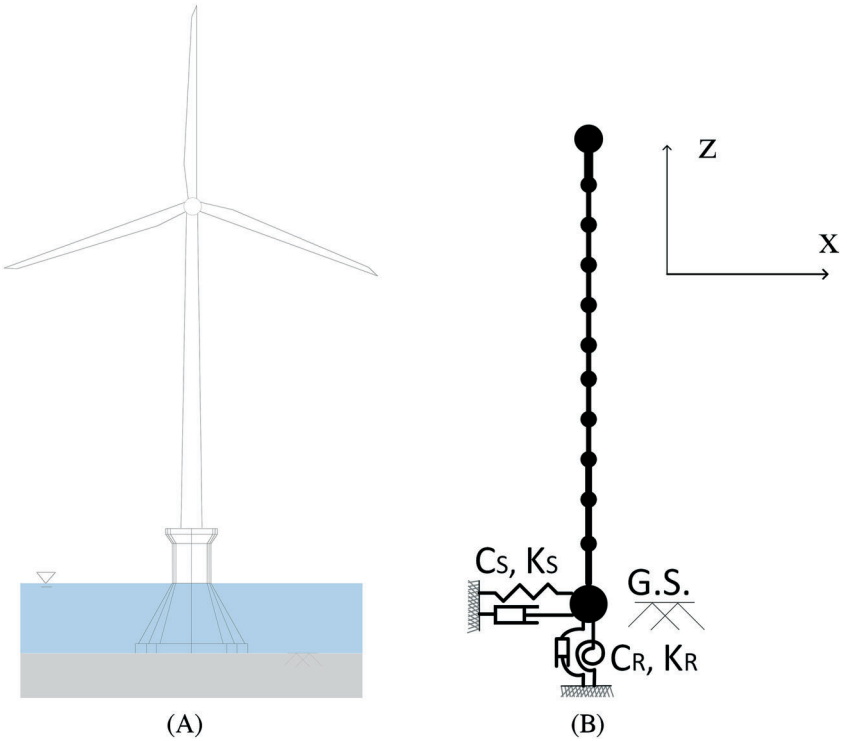

FIGURE 1 Gravity foundation–supported offshore wind turbine: A, wind turbine; B, sway-rocking model [Colour figure can be viewed at wileyonlinelibrary.com]

$$K_S = K_{S0}^{real} \cdot G_e \cdot L_0,\ C_S = \frac{K_{S0}^{imag} \cdot G_e \cdot L_0}{\omega}, \tag{2}$$

$$K_R = K_{R0}^{real} \cdot G_e \cdot (L_0)^3,\ \ C_R = \frac{K_{R0}^{imag} \cdot G_e \cdot (L_0)^3}{\omega}, \tag{3}$$

where K_{j0}^{real} and K_{j0}^{imag} are the real and imaginary parts of $K_{j0}(\omega)$ and j = S and j = R express the sway and rocking motions, respectively. ω is the circular frequency, $L_0 = \frac{\sqrt{\pi r_0^2}}{2}$, $r_0 = \sqrt{A/\pi}$, and A is the area of foundation. G_e is the equivalent shear stiffness of layered soil and is derived by using Cone model[5] as Equation (4). The cone model was used for the dynamic response of slab footings on an unlayered soil (homogeneous half-space) as shown in Meek and Wolf[15] and on a soil layer resting on rigid rock as shown in Meek and Wolf.[16] The cone model has been extended to multiple soil layers on the elastic bedrock and widely used in seismic engineering as shown in JSCE.[5]

$$G_e = \beta_h G_1. \tag{4}$$

Here,

$$\beta_h = \frac{1}{\sum_{i=1}^{n}(1/\alpha_i)},\ \alpha_i = \left(\frac{G_i}{G_1}\right)\frac{z_i z_{i-1}}{z_0(z_i - z_{i-1})}(i = 1, 2, \ldots, n-1),\ \alpha_n = \left(\frac{G_n}{G_1}\right)\frac{z_{n-1}}{z_0},\ z_0 = \pi r_0 \frac{2-\upsilon_1}{8},\ z_i = z_0 + \sum_1^i h_i,\ G_i = \rho_i V_{s,i}^2,\ \upsilon_i = \frac{1 - 2\left(V_{S,i}/V_{P,i}\right)^2}{2\left\{1 - \left(V_{S,i}/V_{P,i}\right)^2\right\}},$$

where ρ_i, υ_i, $V_{S,i}$, $V_{P,i}$, and h_i are the soil density, Poisson ratio, S-wave velocity, P-wave velocity, and height of ith layer (i = 1,2,...,n), respectively.

K_{j0}^{real} and K_{j0}^{imag} are calculated based on the theory of dynamic ground compliance (DGC) proposed by Kobori.[17] The detail information about how to use DGC to calculate K_{j0}^{real} and K_{j0}^{imag} can be seen in AIJ.[18] Figure 2 shows the relationship of nondimensional dynamic impedance and frequency ($a_0 = \frac{\omega L_0}{V_{Se}}$, $V_{Se} = \sqrt{G_e/\rho_e}$, $\rho_e = \rho_1$) for the case with a Poisson ratio of 0.35 ($\upsilon_e = \upsilon_1$), a damping ratio of 2%, and an aspect ratio of 1.00.

Note that a reduced shear modulus and an increased soil damping should be considered when the soil strain increases. The initial shear modulus and the minimum soil damping of 2% shown in JSCE[5] are used in this study since the loading levels in the excitation tests[3] are low, which is consistent with the recommendation in DNVGL.[19] The contribution of soil damping caused by the high loading level is not discussed in this paper, but it can be considered similarly by using the reduced shear modulus and the enlarged damping as recommended in JSCE.[5]

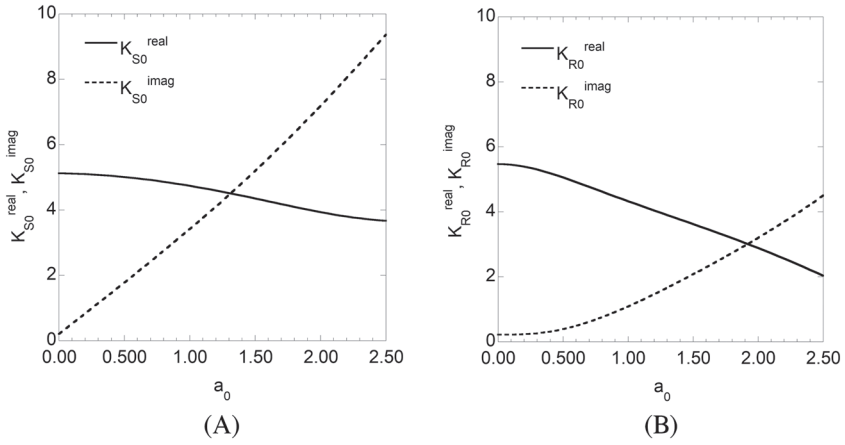

FIGURE 2 Nondimensional dynamic impedance: A, sway motion; B, rocking motion

2.2 | Winkler model for monopile foundation

The monopile foundation supported wind turbine is modelled by a Winkler model, as shown in Figure 3. In Winkler model, the rotor-nacelle assembly is modelled with a lumped mass and connetted to the tower top by using a rigid beam. The tower and the pile are modelled with the lumped masses and the Euler-Bernoulli beam elements. The number of tower beam elements is 24, which follows the suggestion of JSCE.[5] All lumped masses and beam stiffnesses are determined according to the real wind turbine. The structural damping ratio of the first mode is determined according to the empirical formula proposed by Oh and Ishihara.[3] The structural damping ratio of the second mode uses the same value as that of the first mode as recommended by JSCE.[5] The soil-structure interaction is modelled by multiple pairs of springs and dashpots in the sway direction.

The spring stiffness values (K_{Si}) are calculated by using the model proposed by Vesic,[20] and dashpot damping values (C_{Si}) are calculated by using the model proposed by Gazetas and Dobry.[21,22] Detail information can be seen in Equations (5) to (7). One point to note is that radiation damping is frequency-dependent and is negligible for frequencies less than 1 Hz.[10] Because the modal frequencies of the first mode in both fore-aft and

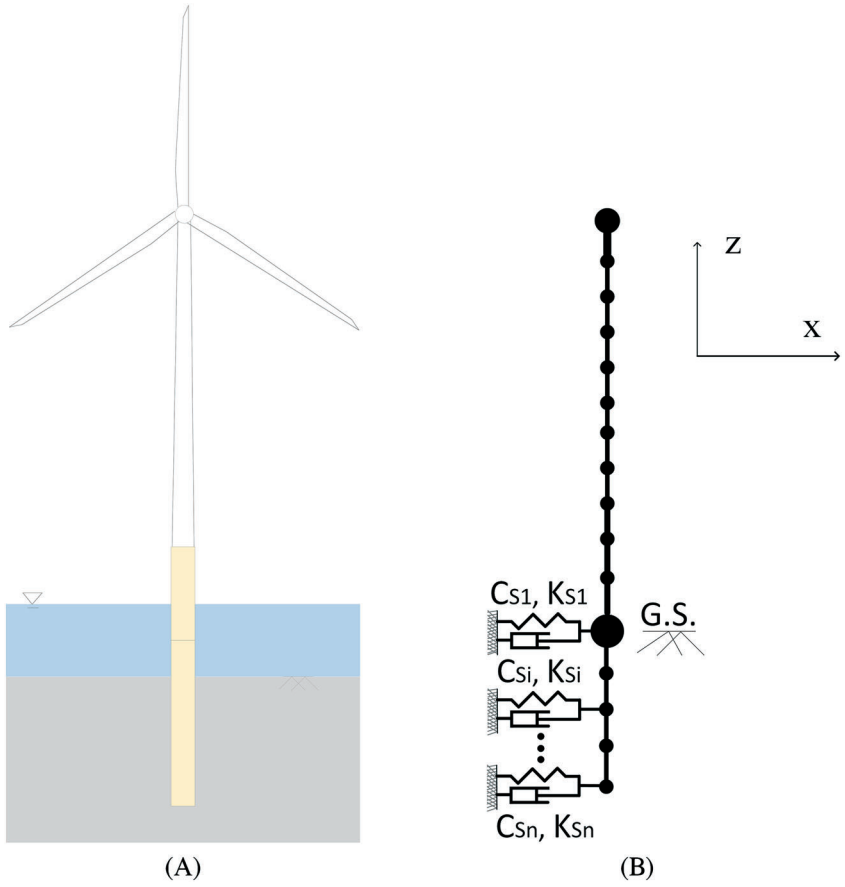

FIGURE 3 Monopile foundation–supported offshore wind turbine: A, wind turbine; B, Winkler model [Colour figure can be viewed at wileyonlinelibrary.com]

side-side directions of MW-size wind turbine are smaller than 1 Hz, radiation damping is neglected for the first mode,[23] which means C_{Si}^{rad} equals to 0 when calculating the modal damping ratio of the first mode. There are many models proposed for the linear soil spring stiffness, such as Vesic,[20] Francis,[24] Roesset,[25] Dobry et al,[26] Kavvadas and Gazetas,[27] and Syngros,[28] among which only the models by Vesic,[20] Francis,[24] and Kavvadas and Gazetas[27] relate the soil spring stiffness to both soil properties (ρ_i, υ_i, $V_{S,i}$, and $V_{P,i}$) and pile properties (E_p, D, I_p, and pile length L). Among these three models, the model proposed by Vesic[20] is the weakest, but it still overestimates the modal frequency and underestimates the modal damping in Section 3.4. That is why the model proposed by Vesic[20] is used in this study.

$$K_{Si} = 0.65\left(\frac{E_i}{1-\upsilon_i{}^2}\right)\sqrt[12]{\frac{E_i D^4}{E_p I_p}},\ E_i = 2(1+\upsilon_i)\rho_i V_{S,i}^2, \tag{5}$$

$$C_{Si} \approx C_{Si}^{hys} + C_{Si}^{rad},\ C_{Si}^{hys} = 2K_{Si}\frac{\beta_i}{\omega},\ C_{Si}^{rad} \approx 2D\rho_i V_{S,i}\left[1+\left(\frac{V_c}{V_{S,i}}\right)^{5/4}\right]a_0^{-1/4}, \tag{6}$$

where C_{Si}^{hys} and C_{Si}^{rad} are hysteretic damping and radiation damping, respectively, $V_c = V_{S,i}\ (z \le 2.5D)$, $V_c = V_{La} = \frac{3.4V_{S,i}}{\pi(1-\upsilon_i)}(z > 2.5D)$, $a_0 = \omega D/V_{S,i}$, E_p, D, and I_p are Young modules, diameter, and moment of inertia of the monopile, respectively, and ρ_i, υ_i, $V_{S,i}$, and $V_{P,i}$ are the same as mentioned above; β_i is the hysteretic damping ratio, and the minimum value is 2% as shown in JSCE.[5] The procedure to calculate β_i is based on Gazetas and Dobry[21] and Damgaard et al[13]: Firstly, a 10-minute transient simulation of the operating wind turbine is conducted by the aeroelastic code FAST.[2] A wind speed level equal to the measured value just before the emergency shutdown is used to determine the load level when the emergency shutdown starts. Secondly, the horizontal pile deformation $y_{d,i}$ in each node depth below the soil surface is determined by performing a static or dynamic deformation analysis using the Winkler model. Thirdly, an equivalent shear strain that yields the same soil material damping can be calculated based on the formula proposed by Kagawa and Kraft[29] as

$$(\gamma_e)_i \approx \frac{1+\upsilon_i}{2.5D}y_{d,i}. \tag{7}$$

Once $(\gamma_e)_i$ is known, the damping ratio β_i can be estimated by a nonlinear soil model. The well-organized Hardin-Drnevich model[30] is used in this study to calculate the damping ratio β_i. As explained in Section 2.1, the contribution of soil damping caused by the high loading level is not discussed in this study.

2.3 | Eigenvalue analysis

Modal frequency and modal shape of each mode can be calculated by eigenvalue analysis. The differential equation for undamped vibrations of a multidegree-of-freedom (MDOF) system is solved.

$$\mathbf{M}\ddot{\mathbf{u}}(t) + \mathbf{K}\mathbf{u}(t) = \mathbf{0}, \tag{8}$$

where $\mathbf{M}$ and $\mathbf{K}$ are the mass and stiffness matrices and $\mathbf{u}(t)$ is the displacement vector. In order to find the eigenfrequency f_j for the jth eigenmode $\mathbf{\Phi}^{(j)}$, a harmonic function is applied as a solution to Equation (8).

$$\mathbf{u}(t) = \mathbf{\Phi}^{(j)}e^{i\omega_j t},\ \omega_j = 2\pi f_j. \tag{9}$$

Insert Equation (9) into Equation (8) and find the jth eigenfrequency f_j and the corresponding eigenmode $\mathbf{\Phi}^{(j)}$ by solving Equations (10) and (11).

$$\det\left(\mathbf{K} - \omega_j^2\mathbf{M}\right) = 0, \tag{10}$$

$$\left(\mathbf{K} - \omega_j^2\mathbf{M}\right)\mathbf{\Phi}^{(j)} = 0. \tag{11}$$

2.4 | Free decay analysis

Modal damping ratio of each mode can be evaluated by using free decay analysis. The equation of motion for wind turbine can be presented as

$$\mathbf{M}\ddot{\mathbf{u}}(t) + \mathbf{C}\dot{\mathbf{u}}(t) + \mathbf{K}\mathbf{u}(t) = \mathbf{f}(t), \tag{12}$$

where **M**, **C**, and **K** are the mass, damping, and stiffness matrices and **f**(t), **u**(t), $\dot{\mathbf{u}}(t)$, and $\ddot{\mathbf{u}}(t)$ are the force, displacement, velocity, and acceleration vectors, respectively. In this study, the Newmark-beta method is used to solve the equation of motion.

The free decay analysis is performed by exciting the tower with a sinusoidal force wave having the same frequency as the expected mode of the offshore wind turbine, keeping the force for 20 seconds to reduce transient vibrations and then removing the applied force to allow the offshore wind turbine to vibrate freely. The modal damping ratio for the excited vibration mode is then estimated using the envelope function of the free decay vibration as shown in Equation (13). Before applying Equation (13), the Butterworth filter may be needed to get pure free decay vibration of the expected mode.

$$g(t) = \mathrm{A}\exp\left(-\omega_j \xi_j t\right). \tag{13}$$

2.5 | Identification of soil parameters

In some cases, the soil parameters are not fully available. In this study, an identification method is proposed to identify soil parameters by using genetic algorithm (GA)[31] and the measurement data, such as the modal frequencies and modal damping ratios of wind turbine. As a global optimization method, genetic algorithm has been widely applied in a broad spectrum of real-world systems such as Si et al.[32] In this study, it is used to search the optimized unknown soil parameters. The procedure of identification is shown as follows:

Firstly, set the layer height as 1 m and divide the soil profile into N layers uniformly. After finishing the identification, check whether the layer height meets the requirement shown as

$$H \le \frac{V_{S,i}}{M \cdot F_{\max}}, \tag{14}$$

where M is a constant and recommended as 4 to 6 and $F_{\max} = 1/(2\Delta t)$ and Δt is the time increment of the excitation.

Then $V_{S,i}$ and $V_{P,i}$ are initially estimated. For the gravity foundation, $V_{S,i}$ and $V_{P,i}$ for the riprap layer are directly taken the same as those of Naarai layer as shown in Figure 5B. For the monopile foundation, $V_{S,i}$ is estimated by using the Ota-Goto model[5] and $V_{P,i}$ is obtained from $V_{S,i}$ and Poisson ratio υ_i as

$$V_{S,i} = 68.79 N_i^{0.171} H_i^{0.199} EF, \tag{15}$$

$$V_{P,i} = V_{S,i}\sqrt{\frac{2-2\upsilon_i}{1-2\upsilon_i}}, \tag{16}$$

where H_i is the depth of ith layer, E is the coefficient for two typical soil eras, namely, 1 for alluvium and 1.303 for diluvium, and F is the coefficient for different soil types as shown in Table 1. N_i for sand and clay as shown in Figure 9B is estimated from the friction angle ϕ_i and the undrained shear strength $S_{u,i}$ by using the empirical formula proposed by Oosaki[33] as

$$N_i = \begin{cases} \dfrac{\left(\phi_i - 15^\circ\right)^2}{20} & (\text{for sand}) \\ \dfrac{2S_{u,i} - 40}{5} & (\text{for clay}) \end{cases}. \tag{17}$$

Values of F are 1 for firm clay and 1.135 for Reese sand as shown in Table 1. The initial value of E is set as 1, and the initial value of υ_i is set as 0.28.

Thirdly, a numerical model is built based on $V_{S,i}$ and $V_{P,i}$ as explained in Section 2.1 or Section 2.2. Eigenvalue analysis and free decay analysis are carried out to predict modal frequencies and modal damping ratios as presented in Section 2.3 or Section 2.4.

Finally, $V_{S,i}$ and $V_{P,i}$ are obtained through identifying E and υ_i in the Ota-Goto model[5] by GA. The range of E is assumed from 0.7 to 1.3, and υ_i is from 0.2 to 0.49. For the gravity foundation, N_i for the riprap layer is assumed the same as that of Naarai, which is 60 as shown in Figure 5B, and value of F is 1.448 for the small stone as shown in Table 1. For the monopile foundation, N_i and F keep the same as above. During the

TABLE 1 Coefficient F for different soil types

Clay	Silver Sand	Medium Sand	Coarse Sand	Gravel	Small Stone
1.000	1.086	1.066	1.135	1.153	1.448

identification, the fitness function is defined as

$$f_{\mathrm{ft}}(x)=\begin{cases}\sqrt{\sum_x w_x\left(\dfrac{x_{\mathrm{pre}}^k}{x_{\mathrm{mea}}}\right)^2} & x_{\mathrm{pre}}^k < x_{\mathrm{mea}}\\ \sqrt{\sum_x w_x\left(\dfrac{x_{\mathrm{mea}}}{x_{\mathrm{pre}}^k}\right)^2} & x_{\mathrm{pre}}^k \geq x_{\mathrm{mea}}\end{cases},\quad w_x=\frac{|x_{\mathrm{pre}}^0-x_{\mathrm{mea}}|}{x_{\mathrm{mea}}}, \tag{18}$$

where $f_{\mathrm{ft}}(x)$ is the fitness function, w_x is the weight of x, which equals to the initial relative error, x_{pre}^0 is the initial prediction of x, x_{pre}^k is the optimal prediction of x of kth generation, and x_{mea} is the measurement of x from field tests, such as the AMD excitation test and the emergency stop test. x could be the modal frequencies of the first and second modes (f_1, f_2) or the modal damping ratios of the first and second modes (ζ_1, ζ_2). During the identification, the generation k is determined by the criteria of relative error and residual, which are shown as

$$\frac{|x_{\mathrm{pre}}^k-x_{\mathrm{mea}}|}{x_{\mathrm{mea}}} < 5\%, \tag{19}$$

$$\frac{|x_{\mathrm{pre}}^k-x_{\mathrm{pre}}^{k-1}|}{x_{\mathrm{mea}}} < 10^{-3}. \tag{20}$$

The relative error is smaller than 5%, which is a requirement from engineering applications. The residual shows the error between two contiguous generations, which is smaller than 10^{-3} for the convergence requirement. Once the relative error and the residual meet or the generation reaches 20, the iteration will stop. Figure 4 shows the flow chart of identification. In Figure 4, K can be K_{S} and K_{R} in SR model or $K_{\mathrm{S}i}$ in Winkler model, while C can be C_{S} and C_{R} in SR model or $C_{\mathrm{S}i}$ in Winkler model. f can be f_1 and f_2, while ζ can be ζ_1 and ζ_2.

When the identification is finished, the relative root means square error of $V_{\mathrm{S},i}$, labeled as rRMSE ($V_{\mathrm{S},i}$), is used to quantify the quality of initial estimation of soil parameters, which is defined as

$$\mathrm{rRMSE}(y)=\frac{\sqrt{\dfrac{\sum_{i=1}^{Q}\left(y_{\mathrm{pre}}^0-y_{\mathrm{pre}}^{\mathrm{iden}}\right)^2}{Q-1}}}{\dfrac{1}{Q}\sum_{i=1}^{Q}y_{\mathrm{pre}}^{\mathrm{iden}}} \tag{21}$$

where Q is the number of identified soil layers. y_{pre}^0 is the initial guess of y, $y_{\mathrm{pre}}^{\mathrm{iden}}$ is the identified value of y, and y represents $V_{\mathrm{S},i}$.

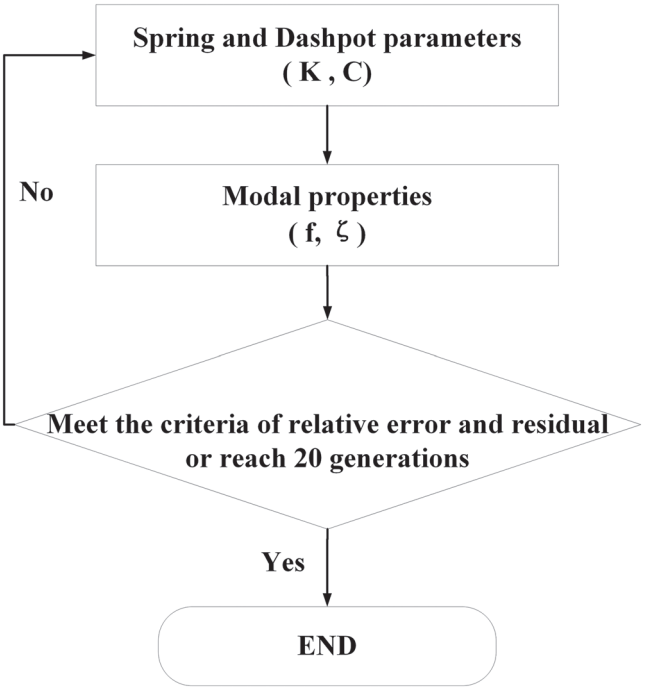

FIGURE 4 Flow chart of the identification procedure

3 | MODAL DAMPING RATIOS FOR WIND TURBINES SUPPORTED BY THE GRAVITY AND MONOPILE FOUNDATIONS

In this section, two offshore wind turbines supported by gravity and monopile foundations are discussed. The wind turbine and soil information for a gravity foundation is first described in Section 3.1, and identification and validation for a gravity foundation–supported wind turbine are investigated by the SR model in Section 3.2. The wind turbine and soil information for a monopile foundation is then presented in Section 3.3, and identification and validation for a monopile foundation supported wind turbine are carried out by the Winkler model in Section 3.4.

3.1 | Wind turbine and soil information for a gravity foundation

The gravity foundation–supported wind turbine in this study is a pitch-regulated MHI 2.4-MW wind turbine located at 3.1 km offshore Choshi, Japan (hereinafter as MHI wind turbine). The outline of MHI wind turbine is shown in Figure 5A. The hub height is 80 m above sea level, and the rotor diameter is 92 m. The wind turbine and the steel tower are supported by a gravity foundation up to 10.83 m above sea level. Detailed information of wind turbine is shown in Table 2. A series of excitation tests using an active mass damper were performed to evaluate the strutural parameters of the targeted offshore wind turbine. The measured modal frequencies and modal damping ratios are shown in Table 3. The measured modal shapes by using five accelerometers are shown in Figure 8. The detail information about the exitation tests can be seen in Oh and Ishihara.[3]

Figure 5B shows the soil profile supporting the gravity foundation. A 2-m riprap layer with the dimension of 30 cm in average is laid under the foundation to make the ground surface flat. The properties of the riprap layer is unknown, which means the identification of soil parameters is necessary. The soil under the riprap layer is a 70-m rock layer, which is referred hereinafter as Naarai layer. Naarai is the name of the soil and distributed throughout Byobugaura seashore, Chiba prefecture. It is a coherent formation and formed by major tuffaceous sandstone and minor

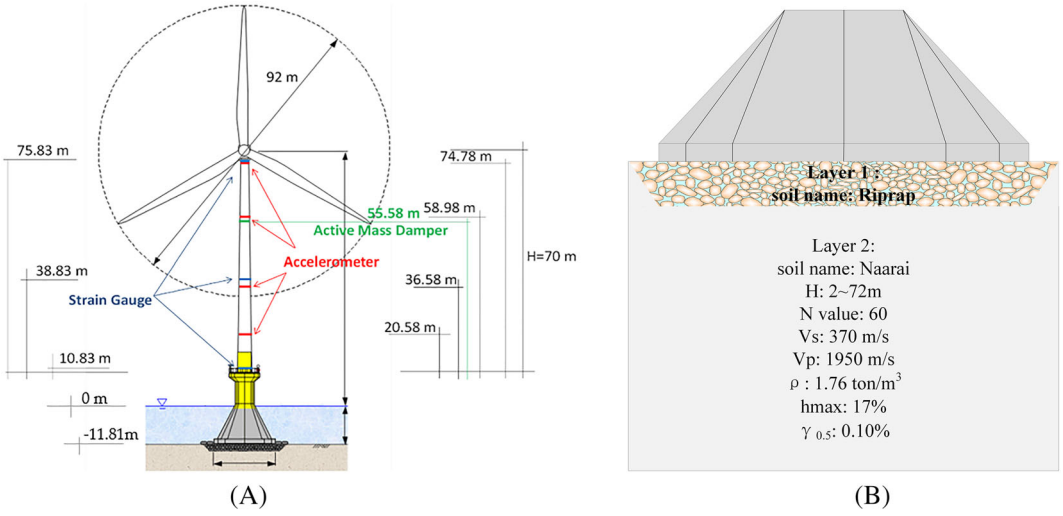

FIGURE 5 Choshi wind power plant: A, outline of the whole system; B, soil information [Colour figure can be viewed at wileyonlinelibrary.com]

TABLE 2 Summary of MHI wind turbine

Description	Value
Rated power	2.4 MW
Hub height (above MSL)	80 m
Rotor, hub diameter	92 m, 4.35 m
Tower diameter, thickness	3.00-4.00 m, 0.022-0.038 m
Nacelle and rotor mass	168 730 kg
Tower mass (with equipments)	360 000 kg
Mean sea level (MSL)	11.81 m
Substructure diameter, wall thickness	6-21 m, 0.5-4.1 m
Substructure height, oblique cone height	22 m, 11 m

TABLE 3 Comparison of measured and predicted modal frequencies and modal damping ratios

	Modal Frequencies			Modal Damping Ratios		
Mode	Measured, Hz	Predicted, Hz	Error, %	Measured, %	Predicted, %	Error, %
First mode	0.350	0.366	4.52	0.200	0.205	2.50
Second mode	2.980	3.154	5.65	2.400	2.400	0.04

silty tuff. The boring test and the ultrasonic test were carried out to obtain the properties of Naarai layer, which are shown in Figure 5B. S-wave velocity and P-wave velocity are constant for the whole Naarai layer, so the $V_{S,i}$ and $V_{P,i}$ for the whole Naarai layer are the same.

3.2 | Identification and validation for a gravity foundation–supported wind turbine

The soil parameters of the riprap layer are identified by using the GA-based identification method. The soil profile under the wind turbine is uniformly divided into 72 layers with the height of 1 m. For the identification, the population is 50, the crossover probability is 0.9, the mutation probability is 0.09, and the generation is 20. The relative error of the modal damping ratios and the modal frequencies of the first and second modes in the identification procedure are shown in Figure 6. It is found that when the generation reaches 20, the relative error of the modal frequency of the second mode is slightly larger than 5%, which may be because of the measurement error or the approximations introduced by the cone model. The initial and identified values of $V_{S,i}$ and $V_{P,i}$ are shown in Figure 7. The initial estimation of $V_{S,i}$ for the riprap layer is 370 m/s, while the identified $V_{P,i}$ is 218 m/s. The rRMSE ($V_{S,i}$) for the initial value is 98.6% because the riprap layer is much softer than the Naarai layer.

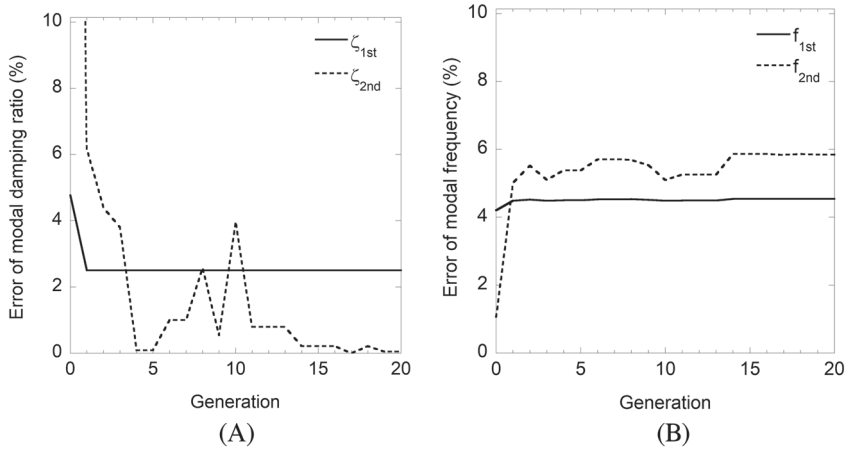

FIGURE 6 Relative error in the identification procedure: A, modal damping ratios; B, modal frequencies

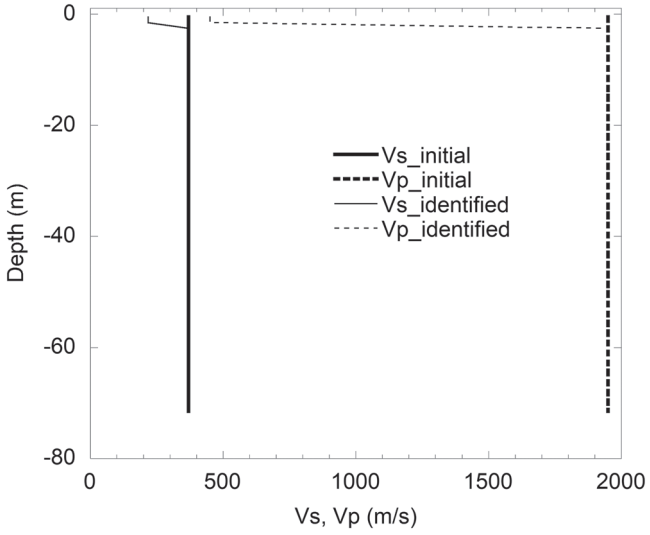

FIGURE 7 Initial and identified soil parameters

Comparisons between the predicted modal frequencies, modal damping ratios, and modal shapes for the first and second modes by using the initial and identified soil parameters and those of measurements are shown in Table 3 and Figure 8. For fitting the modal damping ratio of the second mode, the eighth-order Butterworth filter is used to extract the response of the second mode. The Butterworth filter is applied on the acceleration time series obtained from the free decay analysis, and detail information was mentioned in Oh and Ishihara.[3] It is noticed that the predicted modal frequencies and modal damping ratios for both first and second modes match well with the measurements as shown in Table 3. The predicted modal shapes of the first mode by both SR and FF models match well with the measurements. However, the predicted modal shape of the second mode by the FF model is underestimated since the FF model cannot describe the motion of foundation. The SR model with initial value of riprap also underestimates the modal shape of the second mode because the Riprap layer is much softer than the Naarai layer.

3.3 | Wind turbine and soil information for a monopile foundation

The monopile-supported wind turbine in this study is a Vestas V90 3-MW wind turbine in the Belwind wind farm (hereinafter as Vestas wind turbine). The wind farm is located in the North Sea on the Bligh Bank, 46 km off the Belgian coast. The outline of Vestas wind turbine is shown in Figure 9A. The hub height is 72 m above sea level, and the rotor diameter is 90 m. The wind turbine and the steel tower are supported by a monopile foundation up to 17 m. The wind turbine information is summarized in Table 4. Two different test cases including emergency stop and ambient excitation tests were performed to evaluate the strutural parameters of the targeted offshore wind turbine. Measurements are taken at four levels as shown in Figure 9A by red lines. For the emergency stop case, the wind speed is 6.5 m/s. The measured modal frequencies, modal

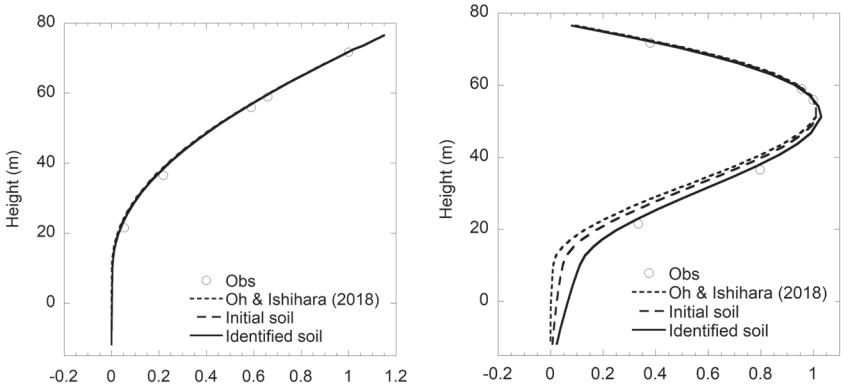

FIGURE 8 Comparison of measured and predicted modal shapes by the identified soil parameters: A, modal shape of the first mode; B, modal shape of the second mode

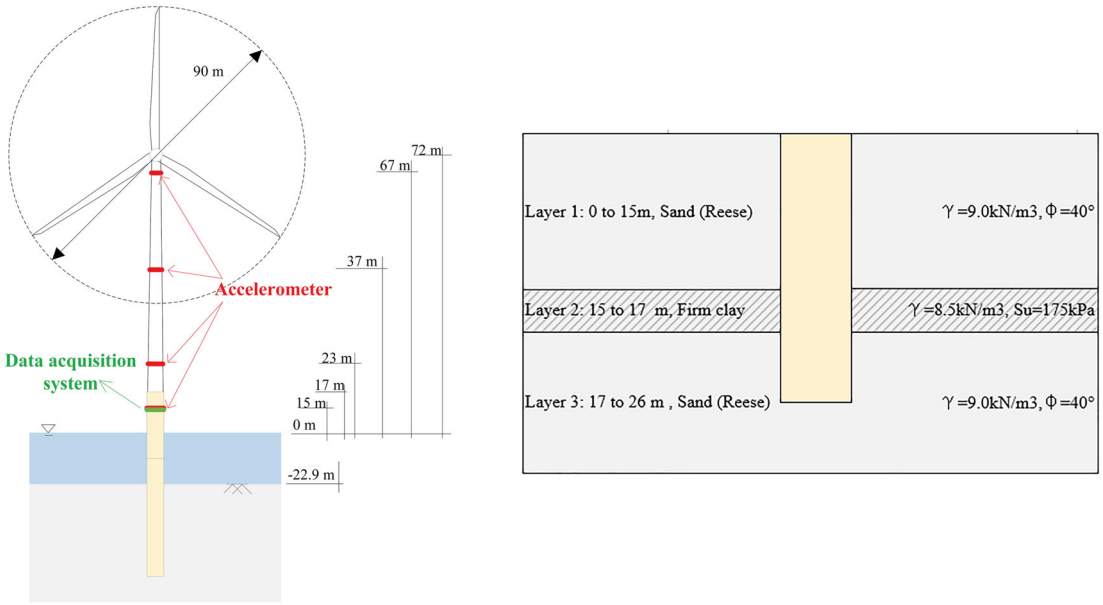

FIGURE 9 Offshore wind turbine supported by monopile foundation: A, outline of the whole system; B, detail information of monopile foundation [Colour figure can be viewed at wileyonlinelibrary.com]

TABLE 4 Summary of Vestas wind turbine

Description	Value
Rated power	3 MW
Hub height (above MSL)	72 m
Rotor, hub diameter	90 m, 2.32 m
Tower diameter, thickness	2.75-4.25 m, 0.013-0.025 m
Nacelle and rotor mass	109 800 kg
Tower mass	108 000 kg
Mean sea level (MSL)	22.9 m
Pile diameter, wall thickness	5 m, 0.07 m
Pile embedded depth	20.6 m

damping ratio, and modal shapes for the this case are shown in Table 5 and Figure 12. The detail information about these exitation tests can be seen in Shirzadeh et al.[14,34]

Figure 9B shows the soil profile supporting the monopile, a 2-m firm clay layer breaks up the continuity of a 24-m stiff sand layer. For the sand layer, the soil density, ρ, and the friction angle, ϕ, are available, while for the clay layer, the soil density, ρ, and the undrained shear strength, S_u, are available. Since $V_{S,i}$ and $V_{P,i}$ are necessary to build the Winkler model, they are identified from the friction angle and the undrained shear strength by using the method shown in Section 2.5.

3.4 | Identification and validation for a monopile foundation supported wind turbine

The soil parameters of stiff sand and firm clay are identified by using the GA-based identification method. The soil profile under the wind turbine is uniformly divided into 21 layers with the height of 1 m. For the identification, the population is 50, the crossover probability is 0.9, the mutation probability is 0.09, and the generation is 20. The relative error of the modal damping ratio of the first mode and the modal frequencies of the first mode and second mode are shown in Figure 10. When the generation reaches 20, the relative errors of the modal frequencies and the modal damping ratios for both first and second modes are under 5%. The initial and identified values of $V_{S,i}$ and $V_{P,i}$ are shown in Figure 11. The initial estimation of $V_{S,i}$ for the top layer is 123 m/s, while the identified $V_{S,i}$ for the top layer is 94 m/s, which leads to the rRMSE ($V_{S,i}$) being 31%. The reason might be that the three-dimensional effect is not included in the initial value of $V_{S,i}$ estimated by Ota-Goto model.

TABLE 5 Comparison of measured and predicted modal frequencies and modal damping ratios

	Modal Frequencies			Modal Damping Ratios		
Mode	Measured, Hz	Calculated, Hz	Error, %	Measured, %	Calculated, %	Error, %
First mode	0.361	0.364	0.83	0.850	0.850	0.00
Second mode	1.560	1.558	0.13	-	14.28	-

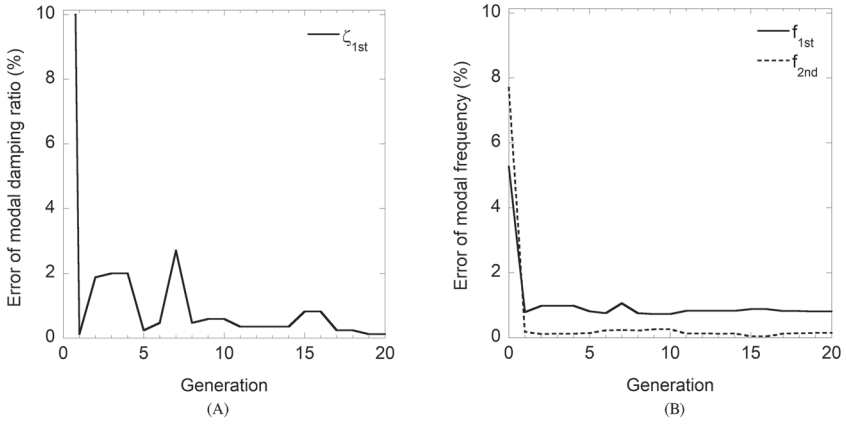

FIGURE 10 Relative error in the identification procedure: A, modal damping ratio; B, modal frequencies

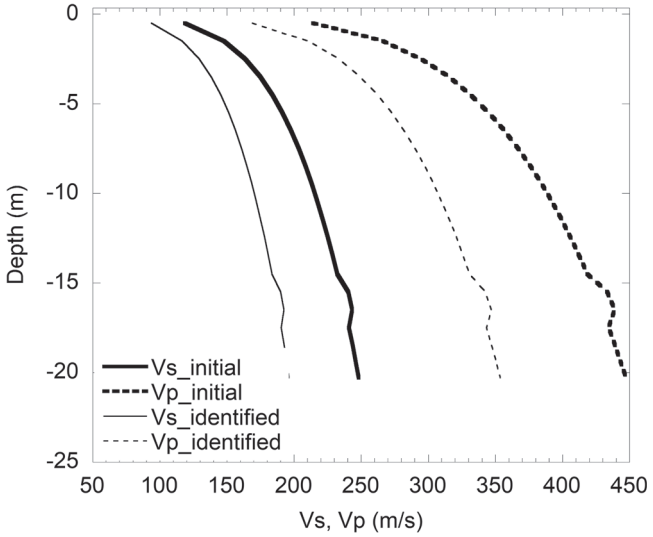

FIGURE 11 Initial and identified soil parameters

Comparisons between the predicted modal frequencies, modal damping ratios, and modal shapes for the first and second modes by using the initial and identified soil parameters and those of measurements are shown in Table 5 and Figure 12. For fitting the modal damping ratio of the second mode, the eighth-order Butterworth filter is also used to extract the response of the second mode. It is found that the predicted modal frequencies for both first and second modes match well with the measurements. The same conclusion can be drawn for the modal damping ratio of the first mode. The predicted modal shapes by both identified soil and initial soil parameters show favorable agreement with the measurements for both first and second modes as shown in Figure 12. The relative error of the predicted modal frequency by the initial soil parameters is 5.3% for the first mode and 7.7% for the second mode as shown in Figure 10B. It is noticed that the modal damping ratio of the second mode is much larger than that of the first mode which was not obtained from the measurements.

4 | EFFECTS OF SOIL PROPERTIES AND FOUNDATION TYPES ON MODAL DAMPING RATIOS

Effect of soil properties on modal damping ratios for the gravity foundation–supported wind turbines is first investigated by a sensitivity analysis study in Section 4.1. The monopile foundation supported wind turbines are then studied in Section 4.2. Finally, a pair of simple models for estimation of the natural period and modal damping ratio of the first mode for both foundations are systematically examined to clarify the effects of soil properties and foundation types on these structural parameters in Section 4.3.

4.1 | Effect of soil properties on modal damping ratios for the gravity foundation–supported wind turbines

A sensitivity analysis study is carried out to investigate the effect of soil properties on the modal damping ratios for the gravity foundation–supported wind turbines. The MHI 2.4-MW offshore wind turbine is installed in Choshi area with different top layers of 2 m and 4 m in depth,

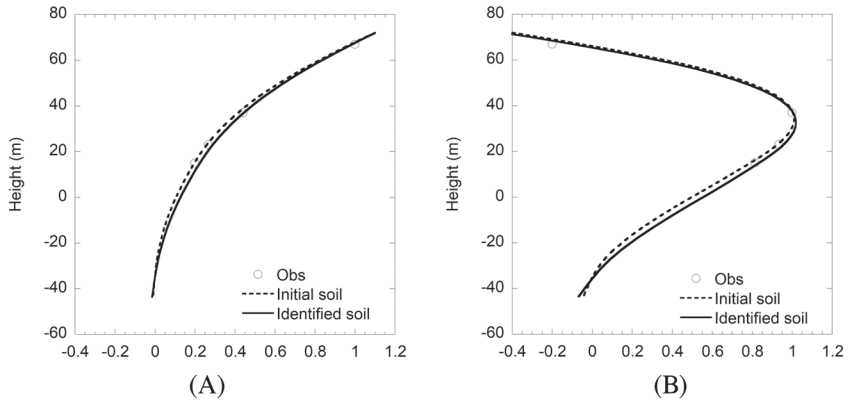

FIGURE 12 Comparison of measured and predicted modal shapes by identified soil: A, modal shape of the first mode; B, modal shape of the second mode

respectively, as shown in Figure 13. For each depth of top layer, Ripraps with a range of average S-wave velocity ($\overline{V}_S$) and a constant Poisson ratio (υ) are used as shown in Table 6. The lower limit of $\overline{V}_S$ is calculated from N value by using Ota-Goto model.[5] N value is determined by JSCE,[5] which suggests that N value of sand and rock should be no less than 20 for the gravity foundation–supported wind turbine. The upper limit of $\overline{V}_S$ is 400 m/s, which is taken as a representative stiffness of engineering bedrock. The soil profile is uniformly divided into 72 layers with the height of 1 m. Since $V_{S,i}$ and $V_{P,i}$ are given, SR model can be built as explained in Section 2.1. Eigenvalue analysis and free decay analysis are carried out to predict modal frequencies and modal damping ratios as presented in Sections 2.3 and 2.4. For fitting the modal damping ratio of the second mode, the 11th-order Butterworth filter is used to extract the response of the second mode.

Figure 14 shows the variation of the modal damping ratios of both first and second modes. The modal damping ratios of the first mode of all cases are close to the structural damping ratio as shown in Figure 14A. This means that soil has little contribution to the modal damping of the first mode for the gravity foundation–supported wind turbine because the rocking motion for the gravity foundation is restricted and will be discussed in Section 4.3. However, the modal damping of the second mode is very sensitive to soil properties and strongly depends on the stiffness of the top layer as shown in Figure 14B. The depth of the top layer has slight effect on the modal damping ratio of the second mode. For $\overline{V}_S$ smaller than 350 m/s, the modal damping ratio of the second mode increases when the depth of the top layer increases. However, for $\overline{V}_S$ larger than 350 m/s, there is little difference in the modal damping ratio of the second mode for the cases with different depths of the top layer. Even though the wind turbine is built on engineering bedrock ($\overline{V}_S$ is 400 m/s), the modal damping ratio of the second mode is 0.75%, which is much larger than the structural damping ratio. The high value of the modal damping ratio of the second mode mainly comes from the contribution of radiation damping, which is negligible for the first mode but is remarkable for the second mode.

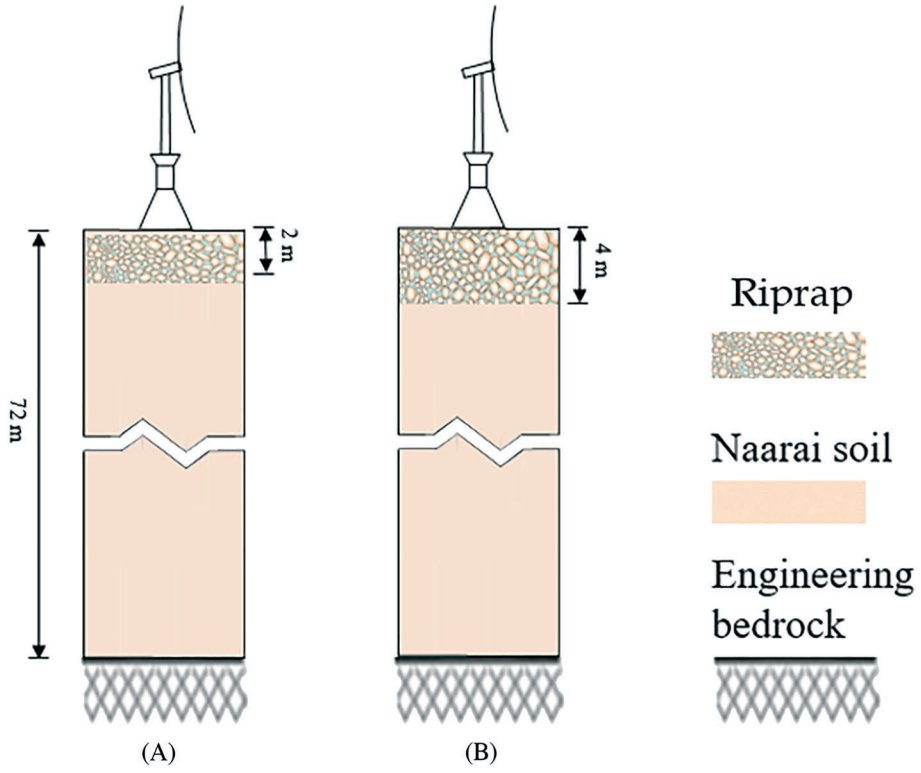

FIGURE 13 Gravity foundation supported wind turbines with 2-m and 4-m top layer depths: A, 2-m top layer; B, 4-m top layer [Colour figure can be viewed at wileyonlinelibrary.com]

TABLE 6 Summary of soil properties and layer thickness

Layer Thickness, m	S-wave Velocity $\overline{V}_S$, m/s	Density ρ, t/m^3	Poisson Ratio, υ	Soil Type
2	130-400	1.76	0.35	Riprap
4	150-400	1.76	0.35	Riprap

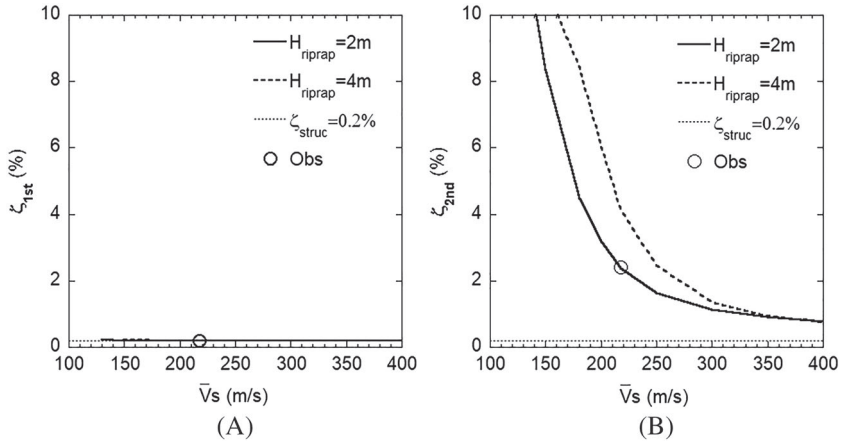

FIGURE 14 Variation of modal damping ratios of first and second modes with the soil stiffness: A, modal damping ratio of the first mode; B, modal damping ratio of the second mode

4.2 | Effect of soil properties on modal damping ratios for the monopile foundation supported wind turbines

A sensitivity analysis study is carried out to investigate the effect of soil properties on the modal damping ratios of the monopile-supported wind turbines with different pile-embedded lengths and different soil properties under the same excitation force, such as the force and moment acting at the pile head caused by a wind speed of 6.5 m/s as shown in Shirzadeh et al.[14] The same Vestas V90 3-MW offshore wind turbine is assumed to be installed in Choshi area with pile-embedded lengths of 20 m and 30 m, respectively as shown in Figure 15; 20-m case is referred to Shirzadeh et al[14] and 30-m case is referred to Damgaard et al.[13] For each pile-embedded length, sands with a range of $\overline{V}_S$ as shown in Table 7 are used. The soil profile is uniformly divided into 20 layers for 20-m case and 30 layers for 30-m case with the height of 1 m. Since $V_{S,i}$ and $V_{P,i}$ are given, Winkler model can be built as explained in Section 2.2. Eigenvalue analysis and free decay analysis are carried out to predict modal frequencies and modal damping ratios as presented in Sections 2.3 and 2.4. For fitting the modal damping ratio of the second mode, the 11th-order Butterworth filter is used to extract the response of the second mode.

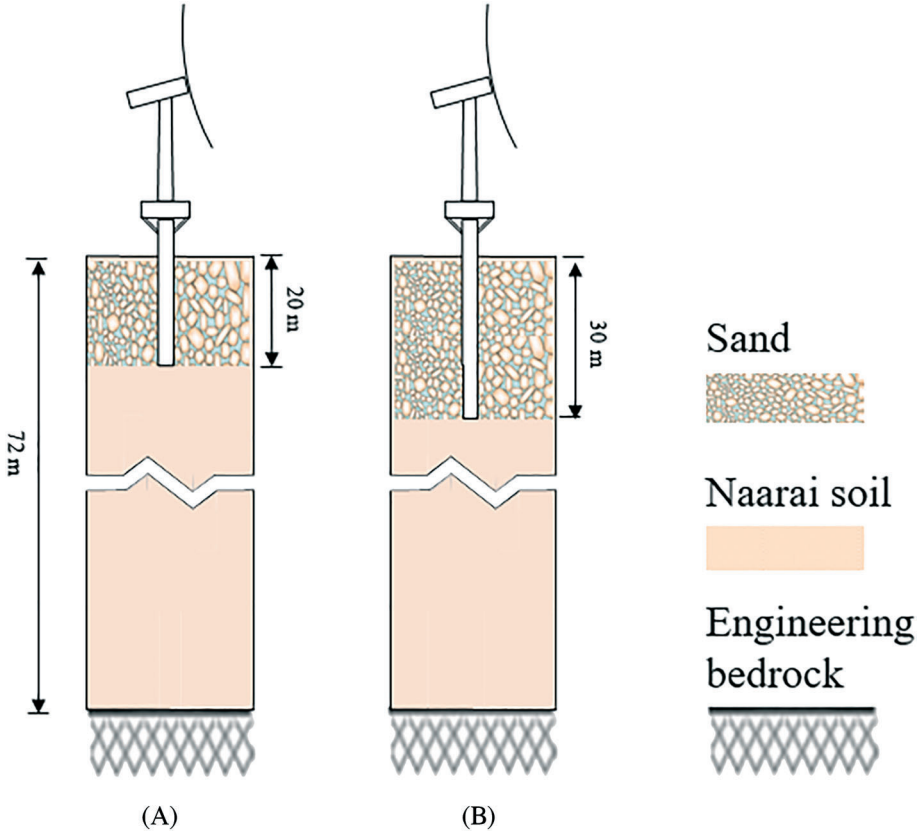

FIGURE 15 Monopile foundation supported wind turbines with 20-m and 30-m pile-embedded lengths: A, 20-m pile; B, 30-m pile [Colour figure can be viewed at wileyonlinelibrary.com]

TABLE 7 Summary of soil properties and monopile length

Monopile Embedded Length, m	S-wave Velocity $\overline{V}_S$, m/s	Density ρ, t/m^3	Poisson Ratio υ	Soil Type
20	100-400	1.94	0.28	Sand
30	100-400	1.94	0.28	Sand

Figure 16 shows the variation of the modal damping ratios for both first and second modes. They are very sensitive to soil properties and significantly depend on the pile-embedded length and the soil stiffness. As shown in Figure 16A, the modal damping ratio of the first mode for 20-m case is larger than that for 30-m case, and the modal damping ratio of the first mode for both cases increases when $\overline{V}_S$ decreases, since the rocking motion for the monopile foundation is allowed and will be analyzed in Section 4.3. The modal damping ratio of the second mode is obviously larger than that of the first mode, but they are reasonable since a value of 7.5% was measured for the modal damping ratio of the second mode for a Vestas V66 2-MW wind turbine embedded in weathered bedrock in Blyth Offshore Wind Farm.[35]

4.3 | Simple models for estimation of natural periods and modal damping ratios of the first mode

Since the dynamic responses of wind turbine under wind and wave are dominated by the first mode, a pair of simple models in AIJ[36] are used to predict the natural period and the modal damping ratio of the first mode for wind turbine and are shown as

$$T_1 = \sqrt{T_{\text{struc,1st}}^2 + T_S^2 + T_R^2}, \tag{22}$$

$$\zeta_1 = \zeta_{\text{struc,1st}}\left(\frac{T_{\text{struc,1st}}}{T_1}\right)^3 + \zeta_S\left(\frac{T_S}{T_1}\right)^3 + \zeta_R\left(\frac{T_R}{T_1}\right)^3. \tag{23}$$

$$\text{Here, } T_S = \frac{2\pi}{\omega_S} = \frac{2\pi}{\sqrt{\frac{K_S}{m_{\text{struc}}}}} = 2\pi\sqrt{\frac{m_{\text{struc}}}{K_S}},\ T_R = \frac{2\pi}{\omega_R} = \frac{2\pi}{\sqrt{\frac{K_R}{I_{\text{struc}}}}} = 2\pi\sqrt{\frac{I_{\text{struc}}}{K_R}},\qquad \zeta_S = \frac{C_S}{2m_{\text{struc}}\omega_S} = \frac{C_S}{2\sqrt{m_{\text{struc}}K_S}},\ \zeta_R = \frac{C_R}{2I_{\text{struc}}\omega_R} = \frac{C_R}{2\sqrt{I_{\text{struc}}K_R}}.$$

$T_{\text{struc,1st}}$ is the natural period of the structure fixed at the base, T_S and T_R are the natural periods of sway and rocking motions assuming the structure is rigid, respectively, and T_1 is the natural period of the first mode of the whole structure, $\zeta_{\text{struc,1st}}$ is the modal damping ratio of the first mode of the structure fixed at the base, ζ_S and ζ_R are the damping ratios of sway and rocking motions assuming the structure is rigid, respectively, and ζ_1 is the modal damping ratio of the first mode of the whole structure. m_{struc} is the whole mass of the structure fixed at the base and I_{struc} is the moment of inertia of the structure fixed at the base. ω_S and ω_R are the circular frequencies of sway and rocking motions, respectively.

The 2-m case of the gravity foundation–supported wind turbine and the 20-m case of the monopile-supported wind turbine are used to evaluate the accuracy of the simple models. Comparisons between the predicted natural periods and modal damping ratios of the first mode for the gravity foundation–supported wind turbine are shown in Figure 17. It is noticed that the predicted natural periods and modal damping ratios of the first mode by two formulae show good agreement with those by numerical simulations. The predicted natural periods and modal damping ratios of

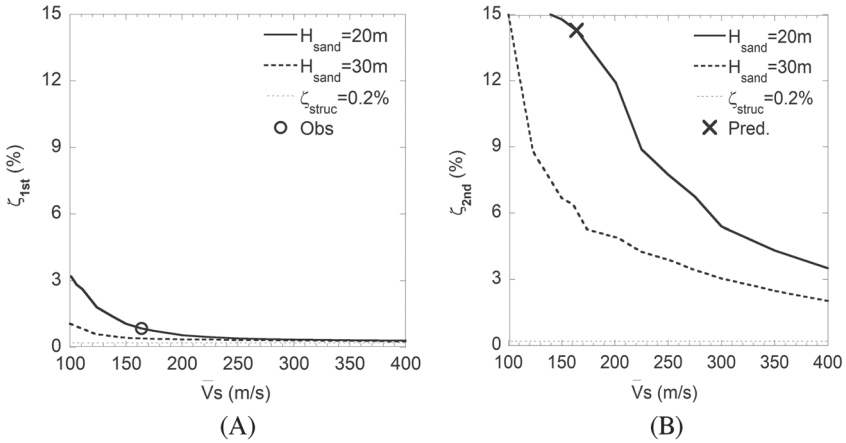

FIGURE 16 Variation of modal damping ratios of first and second modes with the soil stiffness: A, modal damping ratio of the first mode; B, modal damping ratio of the second mode

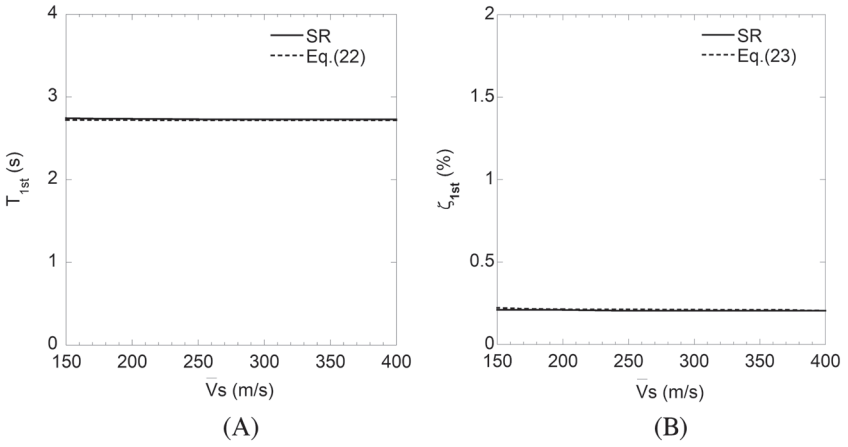

FIGURE 17 Comparisons of the predicted natural period and modal damping ratio of the first mode by formulae and numerical simulations for a gravity foundation supported wind turbine: A, natural period of the first mode; B, modal damping ratio of the first mode

the first mode for the monopile-supported wind turbine are studied by using the equivalent SR model, which can be derived from Winkler model. Detail information are summarized in Appendix A. Comparisons between the predicted natural periods and modal damping ratios of the first mode for the monopile foundation supported wind turbine are shown in Figure 18. It is found that the predicted natural periods and modal damping ratios of the first mode by two formulae show good agreement with those by Winkler model and the equivalent SR model. They indicate that these simple models can be used to predict the natural periods and modal damping ratios of the first mode for wind turbines supported by both gravity and monopile foundations.

Table 8 shows natural periods and modal damping ratios with different soil stiffnesses for a gravity foundation–supported wind turbine. It is noticed that the structural period and damping ratio of superstructure including wind turbine and tower are dominant for the natural period and modal damping ratio for the first mode of the whole structure. This is because the sway motion is strongly restricted by the large friction in the interface between gravity foundation and soil and the rocking motion is prevented by the large horizontal dimensions of gravity foundation.

Table 9 illustrates natural periods and modal damping ratios with different soil stiffnesses for a monopile foundation supported wind turbine. It is found that for the modal damping of the first mode of the whole structure, when the soil is stiff, the superstructure is dominant, the rocking motion contributes the second most, while the contribution from the sway motion is negligible. When $\overline{V}_S$ equals to 400 m/s, the superstructure

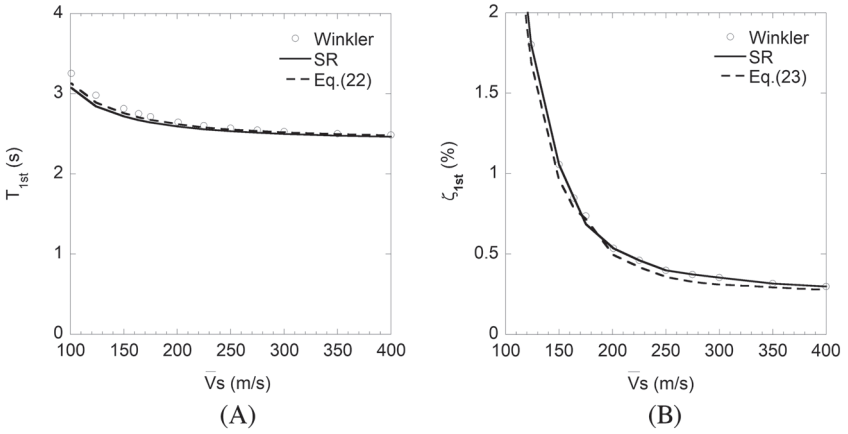

FIGURE 18 Comparisons of the predicted natural period and modal damping ratio of the first mode by formulae and numerical simulations for a monopile foundation supported wind turbine: A, natural period of the first mode; B, modal damping ratio of the first mode

TABLE 8 Variation of periods and damping ratios with soil stiffness for a gravity foundation–supported wind turbine

$\overline{V}_S$, m/s	T_1, s	$T_{struc,1st}$, s	T_S, s	T_R, s	ζ_1, %	$\zeta_{struc,1st}$, %	ζ_S, %	ζ_R, %
150	2.72	2.72	0.24	0.44	0.22	0.20	12.91	3.05
200	2.72	2.72	0.20	0.36	0.21	0.20	15.89	3.62
250	2.72	2.72	0.18	0.31	0.21	0.20	18.78	4.28
300	2.72	2.72	0.17	0.29	0.21	0.20	20.92	4.79
350	2.72	2.72	0.16	0.28	0.21	0.20	22.48	5.19
400	2.72	2.72	0.16	0.27	0.21	0.20	22.99	5.32

TABLE 9 Variation of periods and damping ratios with soil stiffness for a monopile foundation supported wind turbine

$\overline{V}_S$, m/s	T_1, s	$T_{struc,1st}$, s	T_S, s	T_R, s	ζ_1, %	$\zeta_{struc,1st}$, %	ζ_S, %	ζ_R, %
150	2.76	2.29	0.30	1.50	0.96	0.20	25.38	5.01
200	2.62	2.29	0.22	1.25	0.49	0.20	18.19	3.22
250	2.55	2.29	0.18	1.12	0.36	0.20	15.60	2.49
300	2.52	2.29	0.15	1.03	0.31	0.20	15.50	2.25
350	2.50	2.29	0.13	0.98	0.29	0.20	17.24	2.25
400	2.48	2.29	0.12	0.94	0.28	0.20	17.28	2.14

contributes to 71% of the modal damping ratio of the first mode and the contribution from the rocking motion is 29%. However, when $\overline{V}_S$ decreases to 150 m/s, the modal damping ratio of the first mode is almost five times larger than the structural damping ratio and mainly comes from the rocking motion. This is because the monopile is free to rotate at the mudline if the stiffness of soil is small. The contributions from the sway motion to the modal damping of the first mode are always negligible because the sway motion is strongly prevented by the lateral soil resistance along the whole pile.

5 | CONCLUSION

In this study, modal damping ratios of offshore wind turbines supported by the gravity and monopile foundations are systematically studied and validated by the field measurements. Conclusions are summarized as follows:

1. A GA-based identification method is proposed and used to identify soil parameters. Predicted modal damping ratios and modal frequencies as well as modal shapes for the first and second modes by identified soil parameters show good agreement with the field measurements for the gravity foundation–supported wind turbine. The increase of the modal damping of the second mode for the gravity foundation–supported wind turbine comes from the contribution of the riprap layer, which is much softer than the original soil.
2. The damping ratio of the second mode for the monopile foundation supported wind turbine is also evaluated by the identified soil parameters, which could not be estimated by emergency stop. Predicted modal frequencies and modal shapes for the first and second modes as well as modal damping ratio for the first mode by identified soil parameters show good agreement with the field measurements for the monopile foundation supported wind turbine.
3. A sensitivity analysis study is carried out to investigate the effects of soil properties and foundation types on modal damping ratios. For the gravity foundation–supported wind turbine, only the modal damping ratio of the second mode significantly depends on the soil stiffness, while for the monopile foundation supported wind turbine, the modal damping ratios of both modes strongly depend on the soil stiffness.
4. Predicted natural periods and modal damping ratios of the first mode by a pair of simple models agree well with those by numerical models for the offshore wind turbines supported by the gravity and monopile foundations, and the contributions to the modal damping ratio of the first mode from the foundations are clarified by these simple models.

ACKNOWLEDGEMENTS

This research was carried out as a part of the project funded by Shimizu Corporation, Hitachi, Ltd, and ClassNK. The authors express their deepest gratitude to the concerned parties for their assistance during this study.

ORCID

Lilin Wang https://orcid.org/0000-0002-6517-4808

REFERENCES

1. Bossanyi EA. GH Bladed user manual. *Garrad Hassan Bladed*, 2009, 832.
2. Jonkman JM, Buhl Jr ML. FAST user's guide. National Renewable Energy Laboratory, Golden, CO, Technical Report No. NREL/EL-500-38230, 2005.
3. Oh S, Ishihara T. Structural parameter identification of a 2.4 MW bottom fixed wind turbine by excitation test using active mass damper. *Wind Energy*. 2018;21(11):1232-1238.

4. American Wind Energy Association and American Society of Civil Engineers. Recommended Practice for Compliance of Large On-land Wind Turbine Support Structures recommended best practice. 2011.
5. Ishihara T. (Ed.), Guidelines for design of wind turbine support structures and foundations, 2010. (in Japanese).
6. IEC61400-1. 4th. edition, Wind turbine generator systems part 1, safety requirements, International Electrotechnical Commission, 2019.
7. Deutsches Institut für Bautechnik. Richtlinie für Windenergianlagen, 2012. (in German)
8. Prowell I. An experimental and numerical study of wind turbine seismic behavior, PhD thesis, University of California San Diego, 2011.
9. Ishihara T, Phuc PV, Fujino Y, Takehara K, Mekaru T. A field test and full dynamic simulation on a stall regulated wind turbine. *Proc APCWE*. 2005;6:599-612.
10. GL WindEnergie. Overall damping for piled offshore support structures, guideline for the certification of offshore wind turbines. Germanischer Lloyd WindEnergie; 2005.
11. Cook MF, Vandiver JK. Measured and predicted dynamic response of a single pile platform to random wave excitation. In: Offshore Technology Conference. Offshore Technology Conference, 1982.
12. Tarp-Johansen NJ, Andersen L, Christensen ED, Mørch C, Frandsen S, Kallesøe B. Comparing sources of damping of cross-wind motion. In: The European Offshore Wind Conference & Exhibition. The European Wind Energy Association, 2009.
13. Damgaard M, Ibsen LB, Andersen LV, Andersen JK. Cross-wind modal properties of offshore wind turbines identified by full scale testing. *J Wind Eng Ind Aerodyn*. 2013;116:94-108.
14. Shirzadeh R, Devriendt C, Bidakhvidi MA, Guillaume P. Experimental and computational damping estimation of an offshore wind turbine on a monopile foundation. *J Wind Eng Ind Aerodyn*. 2013;120:96-106.
15. Meek JW, Wolf JP. Cone models for homogeneous soil. I. *J Geotech Eng*. 1992;118(5):667-685.
16. Meek JW, Wolf JP. Cone models for soil layer on rigid rock. II. *J Geotech Eng*. 1992;118(5):686-703.
17. Kobori T. Dynamic response of rectangular foundations on an elastic-space. *Proceedings of Japan National Symposium on Earthquake Engineering*. 1962.
18. AIJ (Architectural Institute of Japan). Seismic response analysis and design of buildings considering dynamic soil-structure interaction. 2006 (in Japanese).
19. DNVGL-ST-0126. Support Structures for Wind Turbines. Oslo, Norway: DNV, 2016.
20. Vesic AB. Bending of beams resting on isotropic elastic solid. *J Eng Mech Div*. 1961;87(2):35-54.
21. Gazetas G, Dobry R. Horizontal response of piles in layered soils. *J Geotech Eng*. 1984;110(1):20-40.
22. Gazetas G, Dobry R. Simple radiation damping model for piles and footings. *J Eng Mech*. 1984;110(6):937-956.
23. Carswell W, Johansson J, Løvholt F, et al. Foundation damping and the dynamics of offshore wind turbine monopiles. *Renew Energy*. 2015;80:724-736.
24. Francis AJ. Analysis of pile groups with flexural resistance. *J Soil Mech Found Div ASCE*. 1964;90(3):1-32.
25. Roesset JM. Stiffness and damping coefficients of foundations. Special Technical Publication on Dynamic Response of Pile Foundations: Analytical Aspects, ASCE, O'Neill and Dobry, eds., 1980
26. Dobry R, O'Rourke MJ, Roesset JM, Vicente E. Horizontal stiffness and damping of single piles. *J Geotech Eng Div*. 1982;108:439-459.
27. Kavvads M, Gazetas G. Kinematic seismic response and bending of free-head piles in layered soil. *Geotechnique*. 1993;43(2):207-222.
28. Konstantinos S. Seismic response of piles and pile-supported bridge piers evaluated through case histories. PhD Thesis. City University of New York, 2004.
29. Kagawa T, Kraft LM. Lateral load-deflection relationships of piles subjected to dynamic loadings. *Soils Found*. 1980;20(4):19-36.
30. Hardin BO, Drnevich VP. Shear modulus and damping in soils: design equations and curves. *J Soil Mech Found Div, Proc ASCE*. 1972;98(sm7):667-692.
31. https://en.wikipedia.org/wiki/Genetic_algorithm
32. Si Y, Karimi HR, Gao H. Modelling and optimization of a passive structural control design for a spar-type floating wind turbine. *J Eng Struct*. 2014;69:168-182.
33. Osaki Y. *Foundations for buildings*. Tokyo, Japan: Gihodo Shuppan; 1991.
34. Shirzadeh R, Weijtjens W, Guillaume P, Devriendt C. The dynamics of an offshore wind turbine in parked conditions: a comparison between simulations and measurements. *Wind Energy*. 2015;18(10):1685-1702.
35. Camp TR, Morris MJ, Van Rooij R, et al. Design methods for offshore wind turbines at exposed sites. Final report of the OWTES project, Garrad Hassan and Partners Ltd., Bristol, UK, 2003.
36. AIJ (Architectural Institute of Japan). *Recommendations for loads on buildings*. Tokyo: Architectural Institute of Japan; 2015.
37. Jalbi S, Shadlou M, Bhattacharya S. Practical method to estimate foundation stiffness for design of offshore wind turbines. In: *Wind Energy Engineering, A handbook for onshore and offshore wind turbines*. United States: Academic Press; 2017:329-352.

How to cite this article: Ishihara T, Wang L. A study of modal damping for offshore wind turbines considering soil properties and foundation types. *Wind Energy*. 2019;1–19. https://doi.org/10.1002/we.2401

APPENDIX A

An equivalent SR model derived from Winkler model

The derivation of the stiffness values of springs can be found in Jalbi et al,[37] and the derivation of the damping values of dashpots is proposed by the authors. The details are given as follows:

Firstly, apply a unit force at the mudline in Winkler model to get the horizontal and rotational displacements (c_{hh}, c_{rh}) and apply a unit moment at the mudline in Winkler model to get the horizontal and rotational displacements (c_{hr}, c_{rr}).

Then assemble the horizontal and rotational displacements into the flexibility matrix $[C] = \begin{bmatrix} c_{hh} & c_{rh} \\ c_{hr} & c_{rr} \end{bmatrix}$ and derive the stiffness matrix $[K] = \begin{bmatrix} 1/c_{hh} & 1/c_{rh} \\ 1/c_{hr} & 1/c_{rr} \end{bmatrix}$. Here, $K_S = 1/c_{hh}$ and $K_R = 1/c_{rr}$ are the springs in the equivalent SR model.

Finally, derive the damping values by Equations (A1) and (A2).

$$C_S = 2K_S\frac{\beta}{\omega_1} = K_S\frac{\beta}{\pi f_1}, \tag{A1}$$

$$C_R = 2K_R\frac{\beta}{\omega_1} = K_R\frac{\beta}{\pi f_1}, \tag{A2}$$

where f_1 is the frequency of the first mode of Winkler model and β is a coefficient, which is similar to soil damping ratio. The damping form is assumed the same as that in Winkler model, and β is identified by equalizing the first mode damping ratios in Winkler model and the equivalent SR model.